Journal of Geochemical Exploration xxx (2008) xxx–xxx

Contents lists available at ScienceDirect

Journal of Geochemical Exploration

journal homepage: www.elsevier.com/locate/jgeoexp

Application of singularity mapping technique to identify local anomalies using stream sediment geochemical data, a case study from Gangdese, Tibet, western China

Renguang Zuo [a,b,c,*], Qiuming Cheng [a,b,c], F.P. Agterberg [d], Qinglin Xia [a,b]

[a] State Key Laboratory of Geological Processes and Mineral Resources, China University of Geosciences, Wuhan, Hubei, 430074, China
[b] The Faculty of Earth Resources, China University of Geosciences, Wuhan, Hubei, 430074, China
[c] Department of Earth and Space Science and Engineering, Department of Geography, York University, Toronto, 4700 Keel Street, Ontario, M3J IP3, Canada
[d] Geological Survey of Canada, 601 Booth Street, Ottawa, Ontario, K1A 0E8, Canada

ARTICLE INFO

Article history:
Received 28 April 2008
Accepted 13 August 2008
Available online xxxx

Keywords:
Multifractal
Singularity
Geochemical anomaly
C–A
Exploration
Tibet

ABSTRACT

Identifying geochemical anomalies from background is a fundamental task in exploration geochemistry. The Gangdese mineral district in western China has complex geochemical surface expression due to complex geological background and was chosen as a study area for recognition of the spatial distribution of geochemical elements and separating anomalies from background using stream sediment geochemical data. The results illustrate that weak anomalies are hidden within the strong variance of background and are not well identified by means of inverse distance weighted; neither are they clearly identified by the C–A method if this method is applied to the whole study area. On the other hand, singularity values provide new information that complements use of original concentration values and can quantify the properties of enrichment and depletion caused by mineralization. In general, producing maps of singularities can help to identify relatively weak metal concentration anomalies in complex geological regions. Application of singularity mapping technique in Gangdese district shows local anomalies of Cu are not only directly associated with known deposits in the central part of the study area, but also with E–W and N–E oriented faults in the north of the study area. Both types of anomalies should be further investigated for undiscovered Cu mineral deposits.

1. Introduction

Separation of anomalies from background values is crucial both in exploration geochemistry and environmental geochemistry. In the past decades, geochemical anomalies have been identified by means of various methods (Harris et al., 1999, 2000). Statistical analysis methods play an important role in separating anomalous values from background values. Conventional statistical methods used for geochemical anomaly separation such as probability graphs, univariate and multivariate analysis methods (Sinclair, 1974; Sinclair, 1976; Sinclair, 1991; Govett et al., 1975; Miesch, 1981; Stanley, 1988; Garrett, 1989; Stanley and Sinclair, 1989; Cheng et al., 1996) are primarily concerned with the frequency distributions of element concentration values and relations among multiple variables. These methods can be regarded as non-spatial statistical tools ignoring the spatial information and spatial autocorrelation structure of the geochemical data. Spatial statistical methods such as moving average technique, kriging and spatial factor analysis (Grunsky and Agterberg, 1988) can take into account spatial correlation and variability within neighboring samples in addition to concentration value frequency distributions and correlation coefficients. These methods may be effective in solving some problems but are of limited use in situations where there is extensive overlap between background and anomalous values, or where weak anomalous values are hidden within the strong variance of background (Cheng, 2007). Anomalous patterns caused by mineralization processes can be highly complex with respect to their spatial and frequency properties. Proper quantification of these spatial and spectral properties can be essential for identification of weak or complex anomalies.

Since Mandelbrot's invention of the concept of fractals more than two decades ago (Mandelbrot, 1977, 1983; Mandelbrot et al., 1984), fractal and multifractal models have been applied to physical and chemical quantities with geometrical support. In the geological sciences, these approaches have been used to describe the irregularity of geological features and the spatial distribution patterns of geological objects (Mandelbrot, 1983; Cheng, 1995; Cheng and Agterberg, 1995; Wang et al., 2006; Wang et al., 2008; Raines, 2008) and to characterize properties of mineralization and mineral deposits, such as grade-tonnage models (Turcotte, 1996, 2002), vein thickness-grade models (Sanderson et al., 1994), accumulative number-deposit and deposit density models (Carlson, 1991; Agterberg et al., 1993; Li

* Corresponding author. State Key Laboratory of Geological Processes and Mineral Resources, China University of Geosciences, Wuhan, Hubei, 430074, China. Tel./fax: +86 27 67883066.
E-mail addresses: zrguang@cug.edu.cn, zrguang1981@126.com (R. Zuo).

0375-6742/$ – see front matter © 2008 Elsevier B.V. All rights reserved.
doi:10.1016/j.gexplo.2008.08.003

et al., 1994; Shi and Wang, 1998). Fractal and multifractal models have also been applied to separate anomalies from background values. Examples include the Concentration–Area model (C–A) (Cheng et al., 1994), Spectrum–Area model (S–A) (Cheng et al., 2000), Multifractal Singular Value Decomposition (MSVD) (Li and Cheng, 2004), Concentration–Distance (C–D) model (Li et al., 2003), mapping singularity technique (Cheng, 2007, 2008) and many other applications (e.g., in the environmental field; Lima et al., 2003, 2008). These methods are gradually being adopted as an effective and efficient means to analyze spatial structures in metallic geochemical systems. In this paper, the singularity mapping technique is demonstrated to be an alternative tool to separate local anomalies from complex geological background. For demonstration purposes, the Gangdese copper mineral district, Tibet, western China, will be studied as an example. The general method of singularity mapping is introduced briefly in the next section for demonstrating how to process the data.

2. Singularity mapping technique

The concept of singularity is used for characterizing the anomalous behaviors of singular physical processes that often result in anomalous amounts of energy release or material accumulation within a narrow spatial–temporal interval (Cheng, 2006, 2007, 2008). Taking hydrothermal mineralization as an example, this event usually occurs within a relatively short period of geological time and causes anomalous enrichment of elements within relatively small volumes of orebodies. From a multifractal point of view, the phenomenon can be described by the following power-law model. Suppose the amount of metal in a volume of rock of size V is written as $\mu(V)$. The metal may occur within an orebody of volume V in a mineralization domain or influence zone of mineralization. The metal concentration for the volume V then can be expressed as $C(V) = \mu(V) / V$. When V changes, the quantities $\mu(V)$ and $C(V)$ change accordingly. For example, when V is reduced, the amount of metal $\mu(V)$ decreases. However, the quantity $C(V)$ will vary depending on properties of the ore. If these are multifractal, the quantities $\mu(V)$ and $C(V)$ follow power-law relationships in V with

$$\mu(V)=cV^{\alpha/3} \tag{1}$$

$$C(V)=cV^{\alpha/3-1} \tag{2}$$

where $\mu(V)$ is the total amount of metal in V, $C(V)$ is the average concentration within V, α is the exponent of the power-law relationship and c is a constant. The index α can be estimated from the values $C(V)$ calculated for different sizes V by means of least squares (LS) fitting of a straight line on log–log paper. The relationships shown in Eqs. (1) and (2) are for three-dimensional (3D) volumes V.

For a 2-D spatial problem, V can be replaced by an area A and metal concentration becomes area concentration. With this notation the power-law relation between $\mu(A)$ (or density $\rho(A)$) and A can be expressed as

$$\mu(A)=cA^{\alpha/2} \tag{3}$$

$$\rho(A)=cA^{\alpha/2-1} \tag{4}$$

The distribution of the singularity α in the mapped area can be described by the fractal dimension spectrum function $f(\alpha)$ which

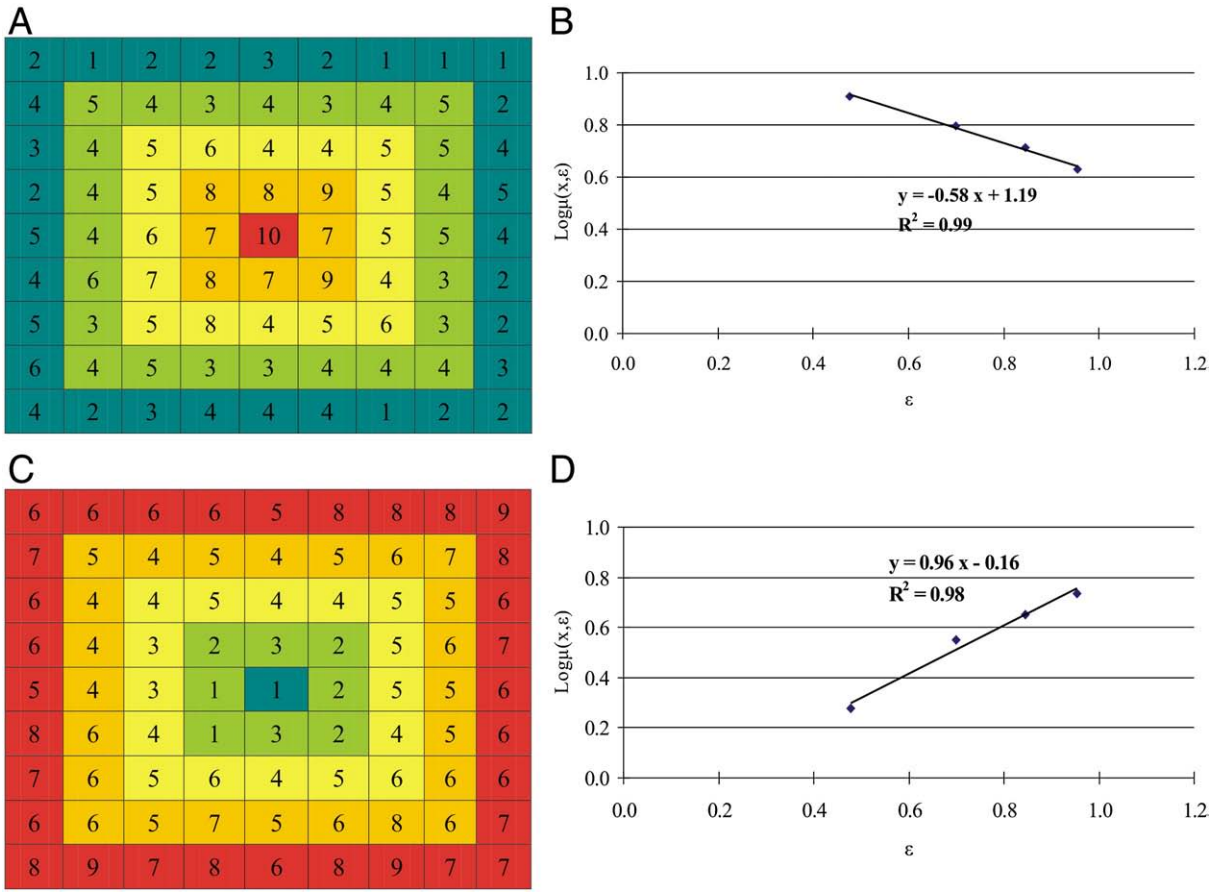

Fig. 1. Illustrations showing data processing by means of window-based method. (A) and (C): box sizes ranging from 3×3, 5×5, 7×7 to 9×9 were used to estimate the average values resulting from enrichment and depletion of the element concentration values, respectively. (B) and (D): two log–log (base 10) plots showing the relationship between the average element concentration values $\mu(x,\varepsilon)$ and box size ε for (A) and (C), respectively, with $\alpha-2$ estimated from slopes of straight lines, that is $\alpha=1.42<2$ for enrichment pattern (A), and $\alpha=2.96>2$ for depletion pattern (C).

Please cite this article as: Zuo, R., et al., Application of singularity mapping technique to identify local anomalies using stream sediment geochemical data, a case study from Gangdese, Tibet, western China, J. Geochem. Explor. (2008), doi:10.1016/j.gexplo.2008.08.003

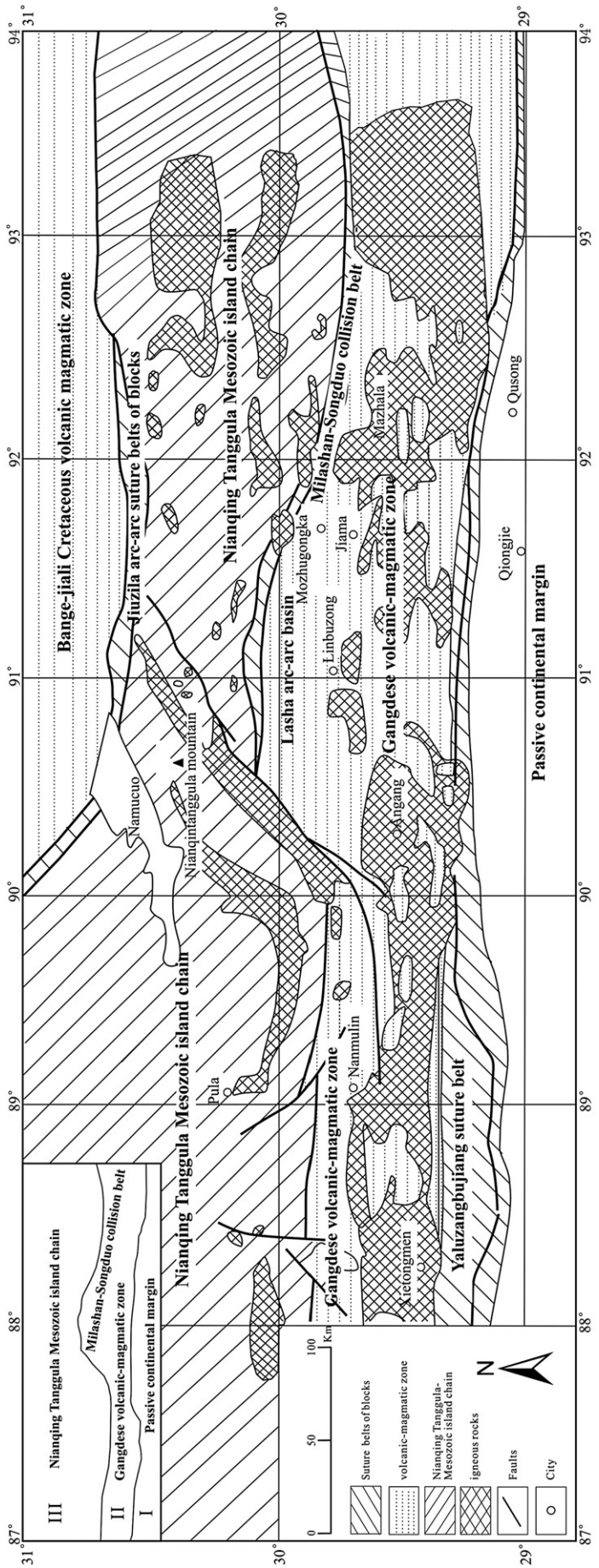

Fig. 2. Simplified geological map, Tibet, west China.

Please cite this article as: Zuo, R., et al., Application of singularity mapping technique to identify local anomalies using stream sediment geochemical data, a case study from Gangdese, Tibet, western China, J. Geochem. Explor. (2008), doi:10.1016/j.gexplo.2008.08.003

Table 1
Statistical properties of geochemical elements

	All zones		I		II		III	
Element	Mean	CV	Mean	CV	Mean	CV	Mean	CV
Ag	0.094	1.519	0.093	2.232	0.091	1.149	0.098	1.261
As	21.147	1.863	25.993	1.762	20.937	2.111	17.403	1.229
Au	2.144	2.173	2.570	1.458	2.322	2.611	1.519	1.451
Cu	26.960	1.136	35.112	0.391	29.287	1.325	16.621	1.397
Hg	0.032	5.525	0.055	5.516	0.025	1.307	0.021	6.971
Mo	1.156	2.338	0.861	0.434	1.444	2.383	0.969	2.575
Pb	28.781	0.980	26.411	0.664	28.969	1.011	30.483	1.090
Sb	1.060	1.488	1.260	1.816	1.091	1.189	0.847	1.360
Sn	3.512	1.511	3.436	0.293	2.961	0.473	4.405	2.144
W	3.288	1.664	2.955	2.242	3.359	1.668	3.461	1.155
Zn	79.062	0.631	89.062	0.268	76.734	0.668	74.189	0.829

Note: CV is coefficient of variances; Ag, Au—ppb, other elements—ppm.

implies that for a conservative field the majority of the area has values of α that are close to 2, whereas the areas with values $\alpha>2$ or $\alpha<2$ are more irregular or unusual (Cheng, 2007, 2008). If element concentration values are considered as realizations of a stationary random variable with a constant population mean, then $\alpha\approx2$ represents non-singularity. "Singular" locations where $\alpha<2$ may indicate abnormal enrichment of the element concentration and these with $\alpha>2$ may indicate element concentration depletion. Further discussion of the existence and property of singularity can be found in Cheng (2007, 2008).

A window-based method can be used for estimating the local singularity from a geochemical map (Cheng, 2006, 2007). It can be described as follows: given a location on the map, define a set of sliding windows $A(r)$ (with square, circular, rectangular, or other shapes) with variable window sizes, $r_{min}=r_1<r_2<\ldots<r_n=r_{max}$, and calculate the average concentration value $C[A(r_i)]$ for each window size. There should be a linear relationship between $C[A(r_i)]$ $(i=1,\ldots,n)$ and r_i, or

$$\mathrm{LogC[A(r_i)]=C+(\alpha-2)Log(r)} \quad (5)$$

The value of $\alpha-2$ can be estimated as the slope from this linear relationship. Then the singularity distribution map can be created by a method similar to the method of sliding windows applied at all locations on the geochemical map. The standard error and squared correlation coefficient involved in the estimation can be calculated from the least squares fitting and these indices can be used for evaluating whether or not the power-law relationships of Eq. (5) exist. The properties of α and data processing are illustrated in Fig. 1.

3. Case study: identification of Cu anomalies in Gangdese, Tibet, west China

3.1. Geological setting

The case study area is located in eastern Tibet, west China. Increasingly attention has been focused on this area because not only are there huge potential mineral resources to be explored, but the area is a natural laboratory for geoscientists to research uplift processes and mechanism of the Qinghai–Tibet plateau. From the Mid–Late Cretaceous the Indus–Yaluzangbo oceanic crust began to be subducted beneath the Lhasa terrane and gave rise to calc-alkaline magmatism in the Gangdese orogenic belt (Allegre et al., 1984), resulting in complex geological background. A simplified geological map is shown in Fig. 2. From south to north, the study area can be divided into three mineralized subzones in terms of their geotectonic background. The first subzone (I) is the passive continental margin, which is located in the southern Brahmaputra Suture Zone. The host rock in this area consists of Triassic to Cretaceous sedimentary rocks (sandstone, mudstone and carbonate) and leucogranites. The second subzone (II) is located in the middle of the study area and occupies most of the Gangdese volcanic–magmatic arc consisting of alkaline lava and intermediate-acid intrusive rocks. The third subzone (III) is located in the northern part of the Gangdese volcanic–magmatic arc and consists of Carboniferous to Permian carbonate rocks with intermediate-acid igneous rocks. The main faults in the study area have E–W, N–E and N–S orientations. These faults systems control the mineralization and distribution of mineral deposits in the study area. The E–W oriented faults control the distribution of porphyry copper deposits from east to west in the middle of the study area, and the faults with N–E and N–S orientations provide favorable conditions for Cu, Mo, Au and other metal deposits (Zuo et al., 2007).

3.2. Copper deposits

Porphyry-type Cu–Mo–Au polymetallic deposits in the study area occur within the Gangdese copper belt, which is about 400 km long and 50 km wide, and the second largest porphyry-type copper belt on the Tibetan plateau after the Yulong copper belt. More than 20 copper deposits including the Zhunuo, Chongjiang, Tinggong, Qulong, and Jiama deposits have been discovered in the study area that is beginning to be recognized as a world-class copper mineralization belt (Hou et al., 2001; Qu et al., 2001). The ore-bearing porphyries of the Gangdese copper belt were formed in the late orogenic stage of the post-collisional evolution history in the Gangdese orogenic belt and had intrusion ages of 18–14 Ma (Qu et al., 2004). The copper deposits are controlled by E–W and N–E oriented faults and the Gangdese magmatic arc, which mainly consists of Late Palaeocene–Early Eocene volcanic rocks and Cretaceous–Tertiary granite batholiths. The mineral assemblages associated with the Cu–Mo–Au mineralization have high concentration values of elements Ag, Au, Cu, Mo, Pb, and Zn (Zuo et al., 2007).

3.3. Stream sediment data and identification of Cu anomalies

The original stream sediment data used in this study comprised of 11 major ore-forming geochemical concentration values of Ag, As, Au, Cu, Hg, Mo, Pb, Sb, Sn, W and Zn were collected and analyzed during the Chinese National Geochemical Mapping (CNGM) project as part of

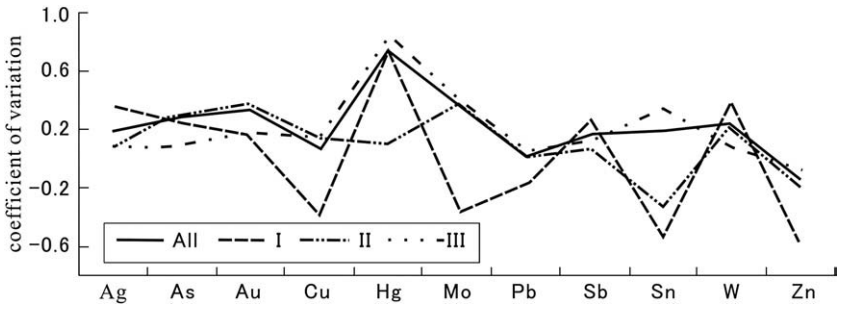

Fig. 3. Different patterns of coefficient of variation (CV) in whole study area and in different subzones (Log base 10).

Please cite this article as: Zuo, R., et al., Application of singularity mapping technique to identify local anomalies using stream sediment geochemical data, a case study from Gangdese, Tibet, western China, J. Geochem. Explor. (2008), doi:10.1016/j.gexplo.2008.08.003

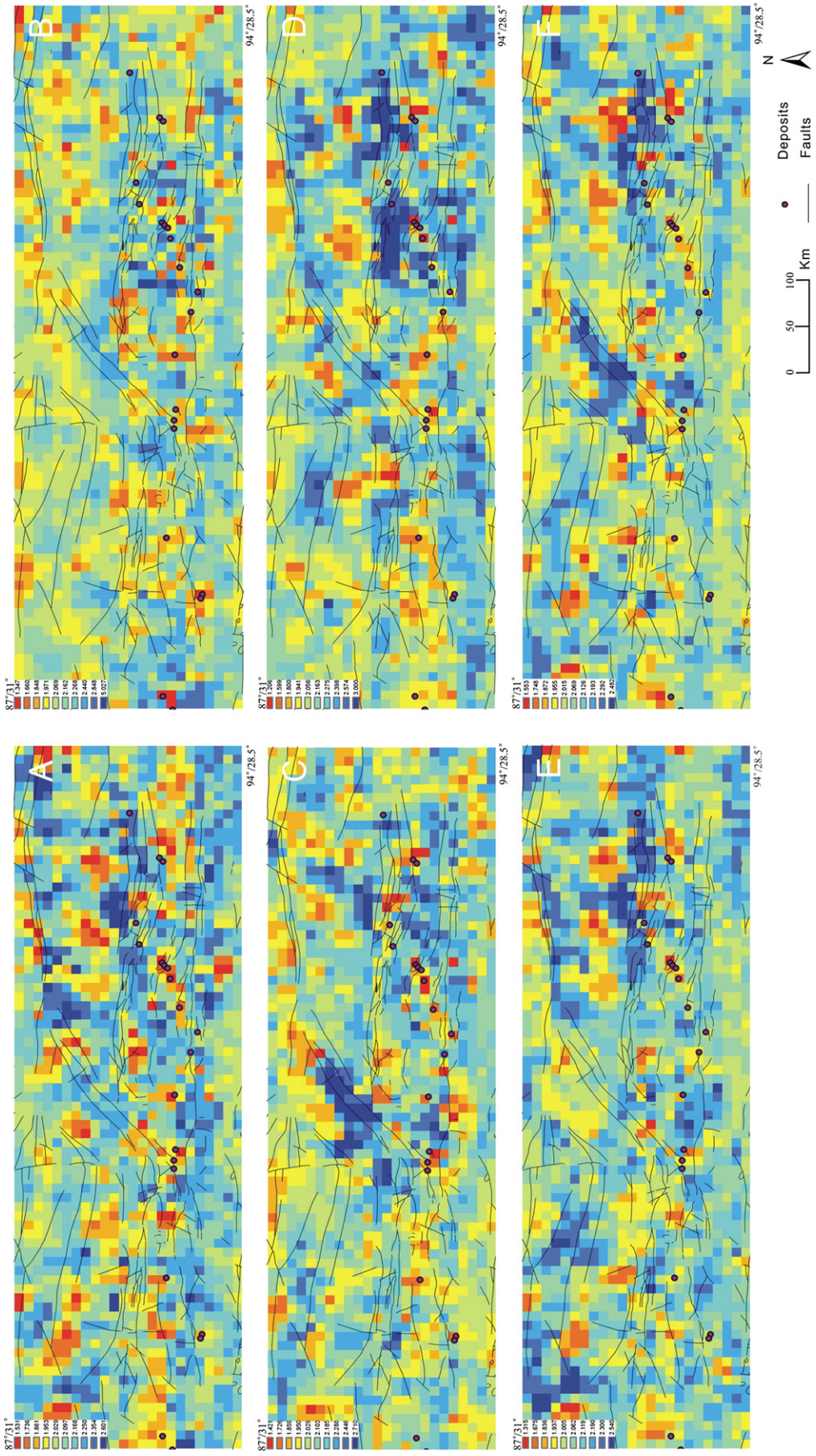

Fig. 4. Estimated singularity α-values by windows-based method: (A) Ag, (B) Au, (C) Cu, (D) Mo, (E) Pb, and (F) Zn.

Please cite this article as: Zuo, R., et al., Application of singularity mapping technique to identify local anomalies using stream sediment geochemical data, a case study from Gangdese, Tibet, western China, J. Geochem. Explor. (2008), doi:10.1016/j.gexplo.2008.08.003

the "Regional Geochemistry National Reconnaissance (RGNR) Project" which was initiated in January 1979 and covered 5.17 million km^2 of China territory with stream sediment sampling and multi-element analysis of 39 major, minor, trace and subtrace elements. Stream sediment samples at a low density of 1 sample per 20–50 km^2 were taken from areas, which are extremely difficult to assess; in other areas, however, a higher density of 1 sample per 4 km^2 was maintained. The multi-elements were mainly analyzed by X-ray Fluorescence (XRF). Further details about the processes involved in sampling and analysis of stream sediment geochemical data can be found in Xie et al. (1997). Statistical properties of geochemical elements are summarized in Table 1 and the coefficients of variation are shown in Fig. 3, indicating different distribution patterns for geochemical concentrations in different subzones.

Values of α were calculated for Ag, Au, Cu, Mo, Pb and Zn using GeoDAS (Cheng, 2000). Seven square windows ranging from 2×2 km^2, 6×6 km^2, 10×10 km^2, 14×14 km^2, 18×18 km^2, 22×22 km^2 to 26×26 km^2 were set. The average value of element concentration $C[A(r_i)]$ can be calculated by averaging the values of all samples falling within a window for each window size. By applying similar processes for each window size centered at the same location, sets of values for average concentration value $C[A(r_i)]$ and size of window r_i (i=1,..., 7) were generated. Log–log plot for these two sets of values show a linear trend, which can be fitted with a straight line by means of the Least Square (LS) method. The slope of this straight line can be taken as the estimated value of $\alpha - 2$, and the standard error and squared correlation coefficient can be calculated to evaluate goodness of fit. Fig. 4A–F illustrates the distributions of α-values estimated by means of this windows-based method for Ag, Au, Cu, Mo, Pb and Zn, respectively. The standard errors and squared correlation coefficients for Cu α-values are shown in Fig. 5, indicating that power-law relationships satisfying Eq. (5) exist with relatively small standard deviations and with all squared correlation coefficients greater than 0.98.

Maps of the distribution of the element concentration values for the whole study area derived by means of the inverse distance weighted moving average method were created by GeoDAS. The moving averaging used a square window of size 8×8 km^2, distance decay exponent 2 and minimum number of samples equal to 12. Fig. 6A–F shows the distribution patterns for Ag, Au, Cu, Mo, Pb and Zn obtained by means of the inverse distance weighted moving average method. Comparing Fig. 4 with Fig. 6, a difference is in the southern area showing strong Cu and Au anomalies in Fig. 6C and Fig. 6B. These anomalies may be caused partly by the high value of geological background concentrations. Anomalies of the same elements in the northern parts of the study area are generally weak. However, these areas have good conditions of mineralization for Cu (Zuo et al., 2007). Clearly, the Cu and Au anomalies in the northern study area could not be identified directly by means of inverse distance weighted.

The weights of evidence method was used for measuring degree of spatial correlation between areas with α-values α<2 and the locations of known mineral deposits with the aid of GeoDAS. This method provides a statistical t-value which measures the significance of spatial correlation between point features and polygons. More details about the method can be found in Bonham-Carter (1994). The larger the t-value is, the stronger the spatial correlation will be. Usually t-value = 1.96 at 95% confidence interval can be accepted as the threshold above which the correlation can be considered as statistically significant. Fig. 7 shows the plot of α-value versus t-value, indicating that spatial correlation (t-value) increases as α-value increases from 1.2 to 1.7, reaching its maximum t-value (3.51), and then decreases as the α-value further increases. This implies α = 1.7 < 2 is the optimum threshold below

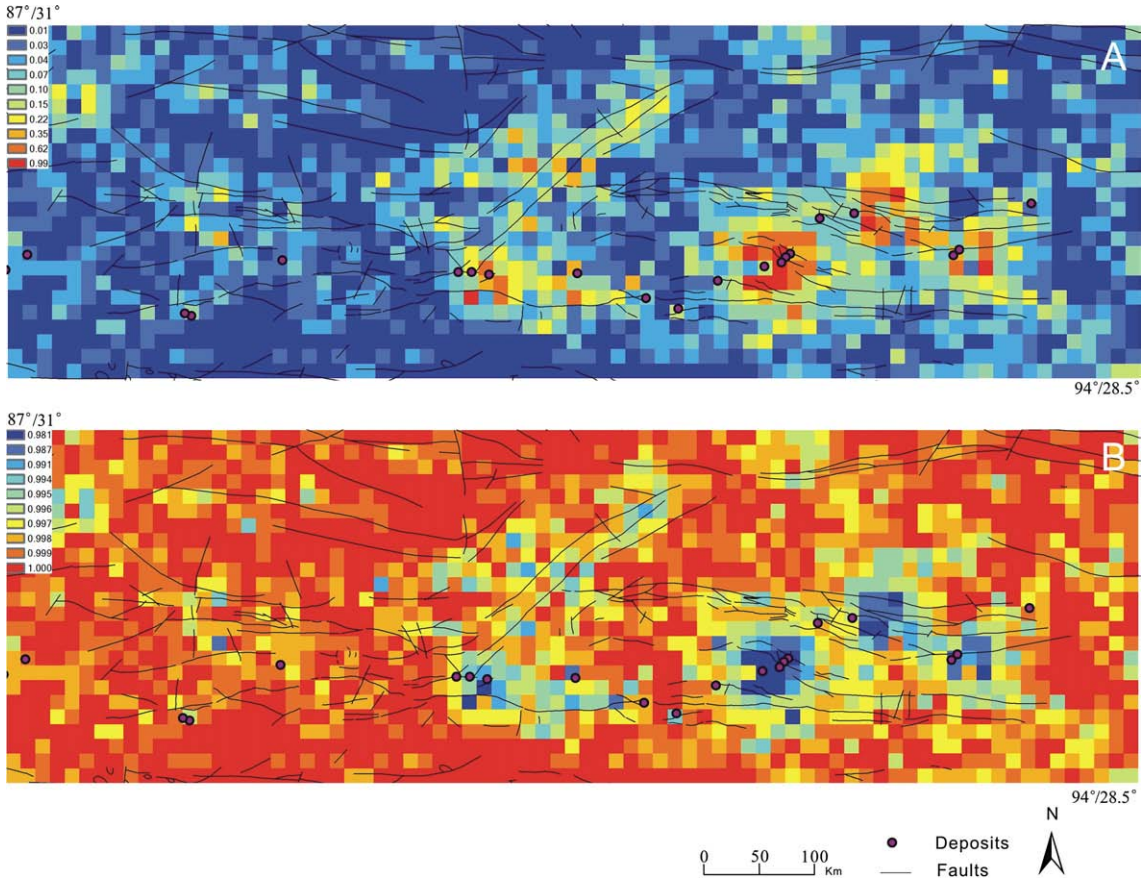

Fig. 5. Standard errors and correlation coefficients for Cu α-values were estimated from least squares fitting. (A) is for standard errors and (B) is for squared correlation coefficients.

Please cite this article as: Zuo, R., et al., Application of singularity mapping technique to identify local anomalies using stream sediment geochemical data, a case study from Gangdese, Tibet, western China, J. Geochem. Explor. (2008), doi:10.1016/j.gexplo.2008.08.003

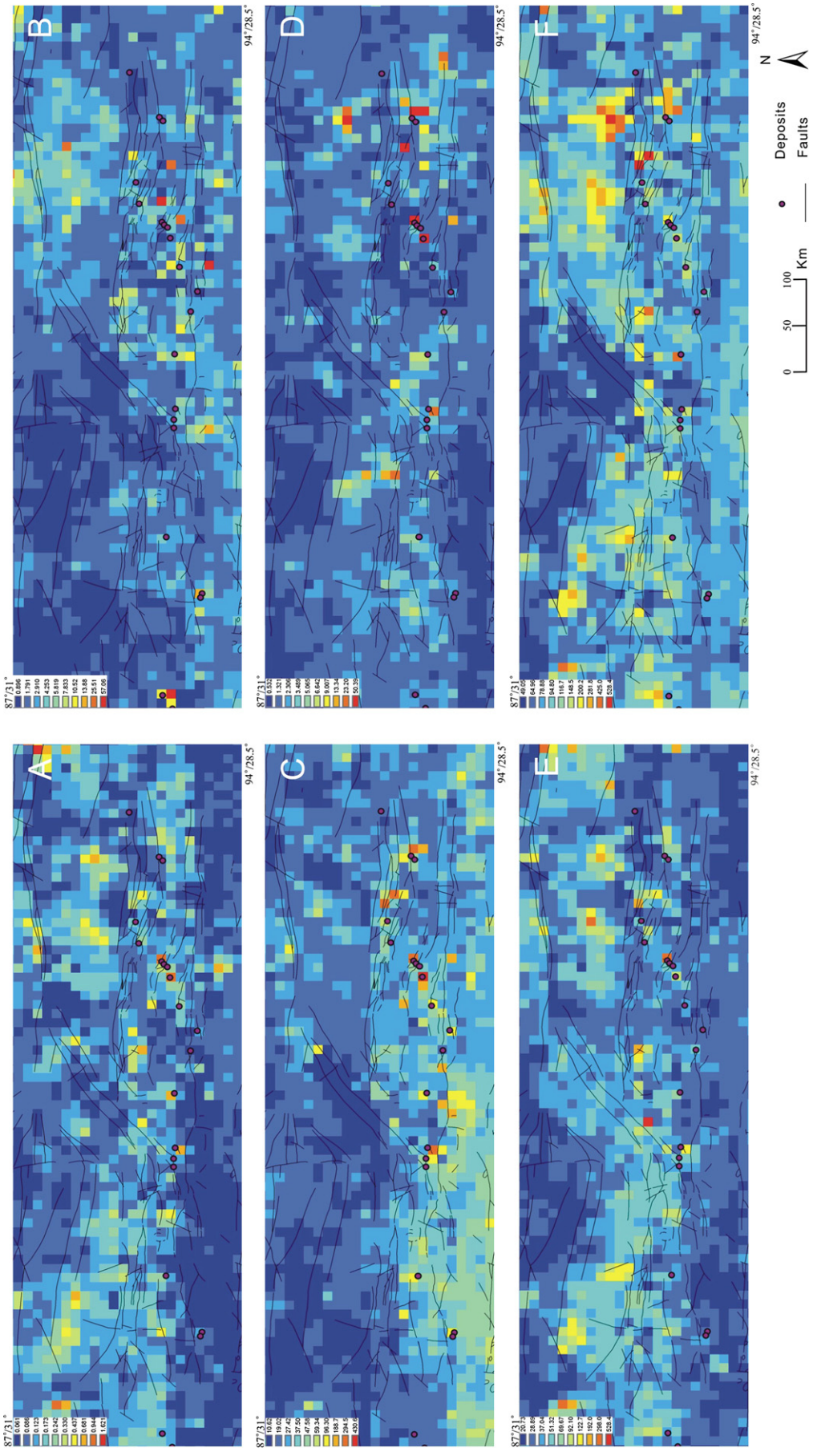

Fig. 6. Maps showing the distribution of (A) Ag, (B) Au, (C) Cu, (D) Mo, (E) Pb and (F) Zn concentration values. Results were created by means of inverse distance weighted moving average method.

Please cite this article as: Zuo, R., et al., Application of singularity mapping technique to identify local anomalies using stream sediment geochemical data, a case study from Gangdese, Tibet, western China, J. Geochem. Explor. (2008), doi:10.1016/j.gexplo.2008.08.003

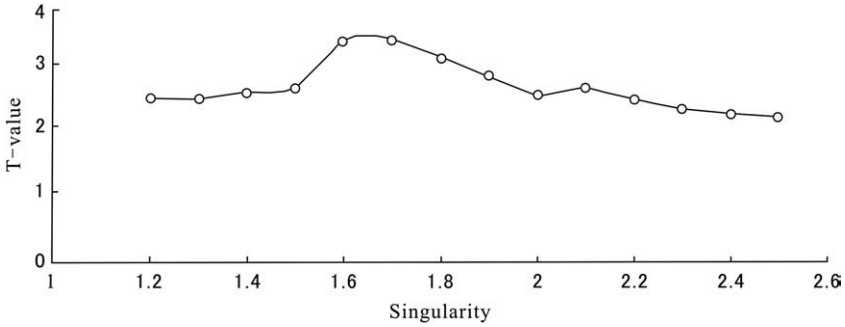

Fig. 7. Student's *t*-value calculated by weights of evidence method for measuring spatial correlation between locations of 20 Cu mineral deposits and areas with α-value below variable thresholds as expressed along *x*-axis. The highest *t*-value (3.51) is reached at $\alpha = 1.7$.

which the area with $\alpha \leq 1.7$ has the highest spatial correlation with the locations of known Cu deposits. The area of $\alpha \leq 1.7$ occupies only 2.4% of the total study area but contains 47.3% of the total number of mineral deposits.

A similar method using weights of evidence was used for evaluating the original concentration value map. The result is shown in Fig. 8. The spatial association index *t*-value reaches its maximum 3.78 at Cu ≥ 59.3 ppm, implying that areas with Cu ≥ 59.3 ppm show significant spatial correlation with the locations of known deposits since the areas with Cu ≥ 59.3 ppm occupy 1.8% of the total study area and contain 42.1% of the total number of mineral deposits.

Fig. 9 shows the target areas for Cu delineated by means of weights of evidence and optimum spatial correlation *t*-value on the basis of singularities with $\alpha \leq 1.7$ (Fig. 9A) and Cu concentration values with Cu ≥ 59.3 ppm (Fig. 9B). Comparing Fig. 9A with Fig. 9B, the main difference is that target areas delineated based on concentration values are mainly located in the southern part of the study area (I), whereas the anomalies delineated by means of the singularity mapping technique are located in the central and northern parts of the study area. The most favorable areas for occurrence of Cu deposits are mainly located in the central zone (II), which has been classified as a porphyry copper deposit zone (Hou et al., 2001; Qu et al., 2001) since more than 20 Cu deposits have already been discovered in it, whereas no Cu deposits have been discovered in subzone I. The Cu anomalies in subzone I in Fig. 9B probably mainly reflect higher background values.

The C–A method proposed by Cheng et al. (1994) was used for separation of anomalies from background. The Fig. 10A–D shows the log–log plots of Cu values versus area for the whole study area, and for subzones I, II and III, respectively. Fig. 11 shows the target areas for Cu delineated on the basis of (A) Cu ≥ 83 ppm (subzone I), Cu ≥ 50 ppm (subzone II), and Cu ≥ 33 ppm (subzone III), and (B) Cu ≥ 40 ppm for the whole study area according to Fig. 10. The targets on Fig. 11A also show significant spatial correlation with the locations of known deposits since their combined area occupies only 2.8% of the total study area but contains 42.1% of the total number of mineral deposits, whereas the targets for Cu in Fig. 11B occupy 10.3% of the total study area but contain 47.3% of the total number of mineral deposits. Comparing Fig. 11A with Fig. 11B, the main difference is that target areas delineated based on whole study area are mainly located in the southern part of the study area (subzone I). The targets in Fig. 11B are similar to those in Fig. 9B, indicating that the C–A method could not clearly identify weak anomalies for the whole study area. However, the target areas for Cu deposits in Fig. 11A are like those in Fig. 9A in the central and northern study area, where the main favorable areas of Cu are located. These results indicate that after dividing the study area into three subzones the weak anomalies could be identified to some extent by means of the C–A method. On the whole, however, the C–A method could not identify local anomalies as clearly as the singularity mapping method (see Fig. 9A), because it resulted in target areas (see Fig. 11A) similar to those in Fig. 9B in the south of the study area (subzone I). However, the C–A method resulted in some weak anomalies in the north of the study area (subzone III) that were not identified by singularity mapping.

4. Conclusions

The Gangdese mineral district has complex geochemical surface expression, resulting from complex and intensive geological events that took place over an extended period of geological time. In such a complex region, if we regard the study area as a whole mineral district regardless of different geological background and different geochemical field, the weak anomalies are not well identified by means of inverse distance weighted and C–A method, because these weak anomalous values are hidden within the strong variance of background. Taking Fig. 11B for the C–A method as an example, almost no Cu anomalies are identified in subzone III characterized by low background value (16.6 ppm, Table 1) and low anomalies (40 ppm, Fig. 11A), because the weak anomalies are hidden within subzone I with high background value (35.1 ppm, Table 1) and high anomalies (83 ppm, Fig. 11A). Two methods could be used for solving these problems. The first consists of dividing the whole study

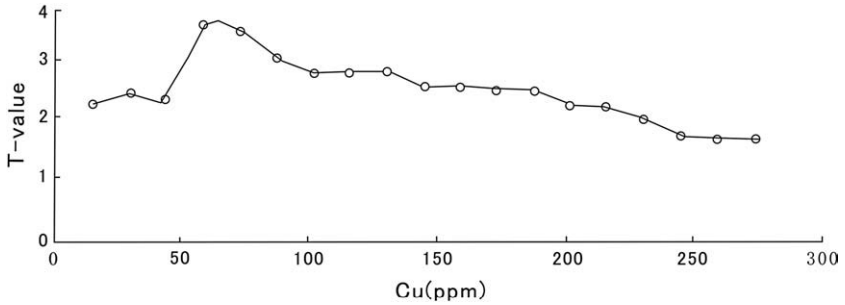

Fig. 8. Student's *t*-value calculated by weights of evidence method for measuring spatial correlation between locations of 20 Cu mineral deposits and the areas with Cu concentration value above variable thresholds as expressed along the *x*-axis. The highest *t*-value (3.78) is reached at Cu = 59.3 ppm.

Please cite this article as: Zuo, R., et al., Application of singularity mapping technique to identify local anomalies using stream sediment geochemical data, a case study from Gangdese, Tibet, western China, J. Geochem. Explor. (2008), doi:10.1016/j.gexplo.2008.08.003

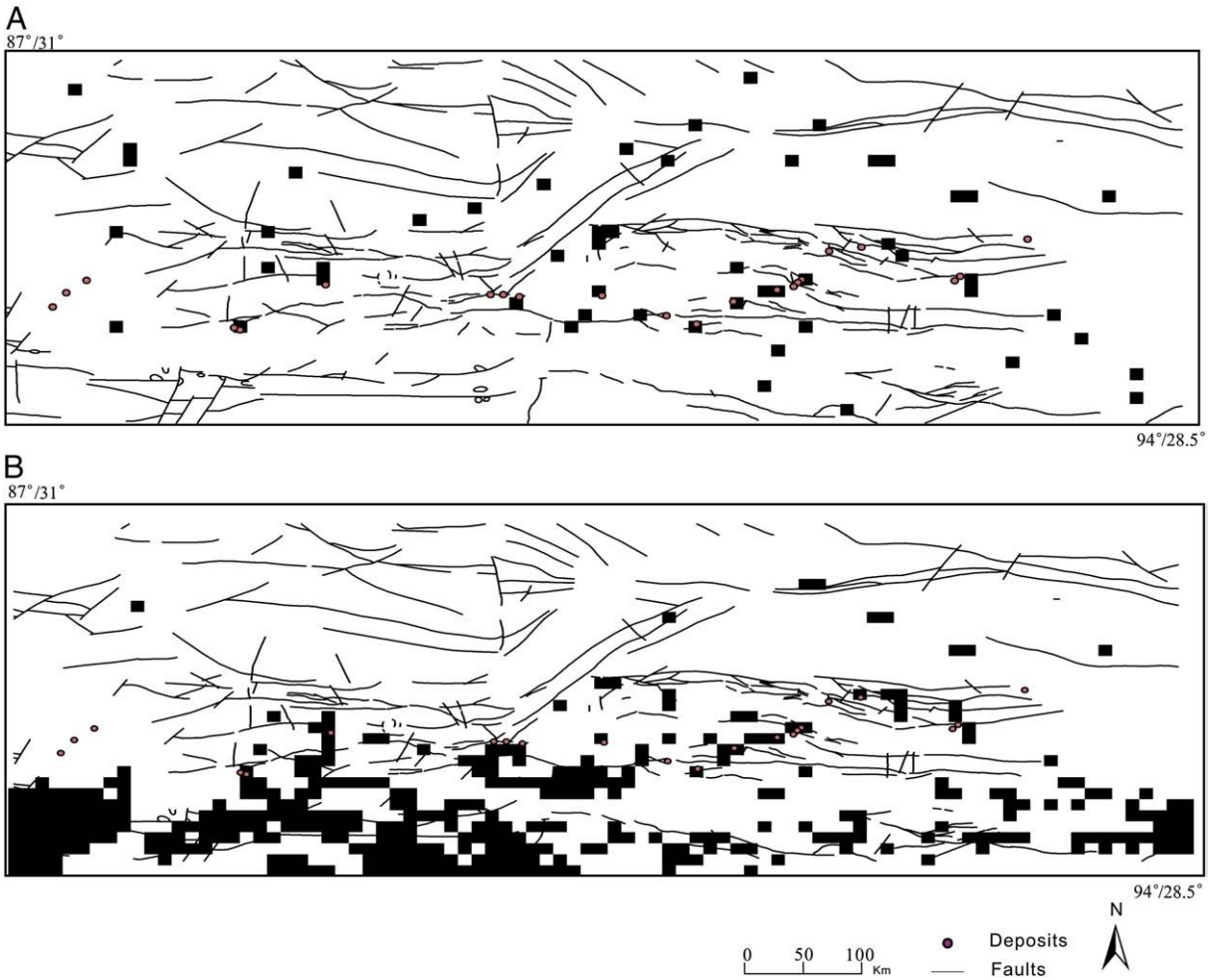

Fig. 9. Targets delineated by means of weights of evidence on basis of (A) singularity of $\alpha \leq 1.7$ and (B) Cu concentration value Cu ≥ 59.3 ppm.

area into subzones in terms of geotectonic background and geochemical field and before identification of anomalies in subzones. However, this method still not clearly identified all local anomalies although it performed relatively well in the northern part of the study area (subzone III). The second method, which is best, is the singularity mapping technique, because it can uncover the local and weak anomalies.

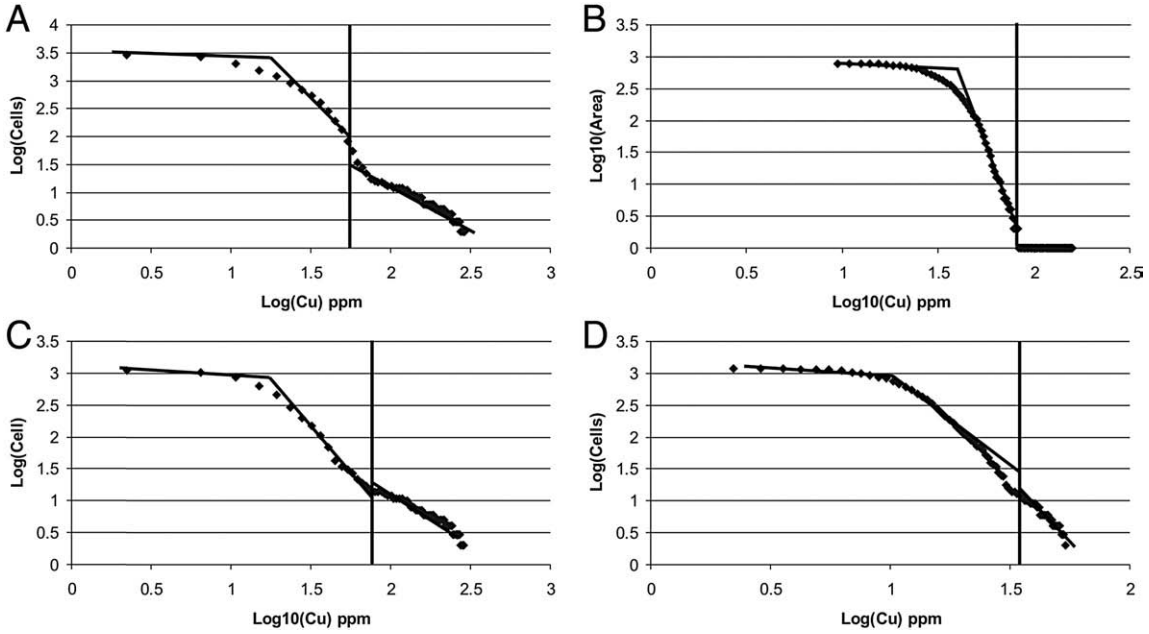

Fig. 10. Log–log plots of Cu value versus area (Log base 10). (A) is for the whole study area; (B) is for I subzone; (C) is for II subzone and (D) is for III subzone.

Please cite this article as: Zuo, R., et al., Application of singularity mapping technique to identify local anomalies using stream sediment geochemical data, a case study from Gangdese, Tibet, western China, J. Geochem. Explor. (2008), doi:10.1016/j.gexplo.2008.08.003

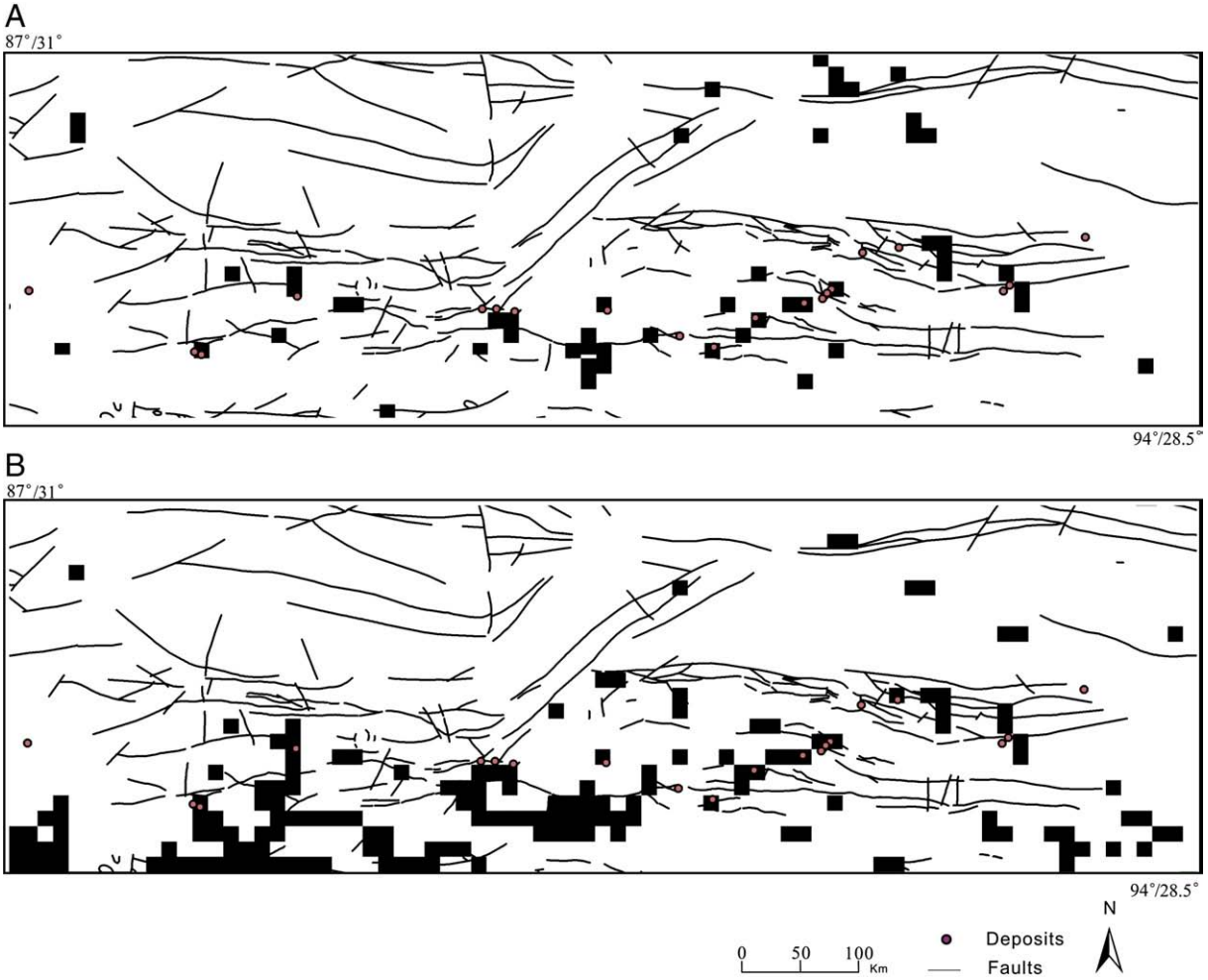

Fig. 11. Targets delineated by means of C–A method on the basis of (A) Cu≥83 ppm (subzone I), Cu≥50 ppm (subzone II), and Cu≥33 ppm (subzone III), and (B) Cu≥40 ppm for the whole study area.

Singularity values may provide new information complementing results based on the original concentration values, and can quantify the properties of enrichment and depletion caused by mineralization. Producing maps of singularities can help to identify relatively weak metal concentration anomalies in complex geological regions. In our case history study, these local anomalies of Cu are not only directly associated with the known deposits in subzone II, but also associated with the E–W and N–E orientations faults in the north of area (subzone III). These anomalies should be further investigated for undiscovered Cu mineral deposits. The method also can be applied in gas and oil exploration.

Acknowledgements

The authors would thank two anonymous reviewers for critical review of the manuscript and constructive comments, and thank the B. De Vivo, Editor-in-Chief of Journal of Geochemical Exploration for constructive suggestions. This research was financially jointed supported by Chinese National Foundation of Science Projects "Distinguished Young Researcher Grant" (40525009) and Strategic Research project (40638041) and National Graduate Student Program of Building World-Class Universities (Grant No:[2007]3020).

References

Agterberg, F.P., Cheng, Q., Wright, D.F., 1993. Fractal modeling of mineral deposits. In: Elbrond, J., Tang, X. (Eds.), Application of Computers and Operations Research in the Mineral Industry: Proc. 24th APCOM Symposium, v. 1: Can. Inst. Mining. Metallurgy and Petroleum Eng. (Montreal), pp. 43–53.

Allegre, C.J., et al., 1984. Structure and evolution of the Himalayan–Tibet orogenic belt. Nature 307, 17–22.

Bonham-Carter, G.F., 1994. Geographic Information Systems for Geoscientists: Modeling with GIS. Pergamon Press, Oxford. 398 pp.

Carlson, C.A., 1991. Spatial distribution of ore deposits. Geology 18, 111–114.

Cheng, Q., 1995. The perimeter-area fractal model and its application to geology. Math. Geol. 27, 69–82.

Cheng, Q., 2000. GeoData Analysis System (GeoDAS) for mineral exploration: user's guide and exercise manual. Material for the Training Workshop on GeoDAS held at York University, Toronto,Canada, vol. 1, 3, p. 204. http://www.gisworld.org/geodas.

Cheng, Q., 2006. Singularity-generalized self-similarity-fractal spectrum (3S) model. Earth Sci.-China Univ. Geosci. 31, 337–348 (in Chinese with English abstract).

Cheng, Q., 2007. Mapping singularities with stream sediment geochemical data for prediction of undiscovered mineral deposits in Gejiu, Yunnan Province, China. Ore Geol. Rev. 32, 314–324.

Cheng, Q., 2008. Non-linear theory and power-law models for information integration and mineral resources quantitative assessments. Math. Geol. 40, 503–532.

Cheng, Q., Agterberg, F.P., 1995. Multifractal modeling and spatial point processes. Math. Geol. 27, 831–845.

Cheng, Q., Agterberg, F.P., Ballantyne, S.B., 1994. The separation of geochemical anomalies from background by fractal methods. J. Geochem. Explor. 51, 109–130.

Cheng, Q., Agterberg, F.P., Bonham-Carter, G.F., 1996. A spatial analysis method for geochemical anomaly separation. J. Geochem. Explor. 56, 183–195.

Cheng, Q., Xu, Y., Grunsky, E., 2000. Multifractal power spectrum–area method for geochemical anomaly separation. Nat. Resour. Res. 9, 43–51.

Garrett, R.G., 1989. A cry from the heart. Explore (AEG Newsl.) 66, 18–20.

Govett, G.J.S., Goodfellow, W.D., Chapman, A., Chork, C.Y., 1975. Exploration geochemistry distribution of elements and recognition of anomalies. Math. Geol. 7, 415–446.

Grunsky, E.C., Agterberg, F.P., 1988. Spatial and multivariate analysis of geochemical data from metavolcanic rocks in the Ben Nevis Area, Ontario. Math. Geol. 7, 415–446.

Harris, J.R., Wilkinson, L., Grunsky, G., et al., 1999. Techniques for analysis and visualization of lithogeochemical data with applications to the Swayze greenstone belt, Ontario. J. Geochem. Explor. 67, 301–334.

Harris, J.R., Grunsky, E.C., Wilkinson, L., 2000. Effective use and interpretation of lithogeochemical data in regional exploration programs. Ore Geol. Rev. 16, 107–143.

Please cite this article as: Zuo, R., et al., Application of singularity mapping technique to identify local anomalies using stream sediment geochemical data, a case study from Gangdese, Tibet, western China, J. Geochem. Explor. (2008), doi:10.1016/j.gexplo.2008.08.003

Hou, Z., Qu, X., Huang, W., 2001. Gangdese porphyry copper belt the second "Yulong" copper belt. China Geol. 28, 27–29–40 (In Chinese with English abstract).
Li, Q., Cheng, Q., 2004. Fractal singular-value (eigen-value) decomposition method for geophysical and geochemical anomaly reconstruction. Earth Sci.-China Univ. Geosci. 29, 109–118 (In Chinese with English Abstract).
Li, C., Xu, Y., Jiang, X., 1994. The fractal model of mineral deposits. Geol. Z. 10, 25–32 (In Chinese with English Abstract).
Li, C., Ma, T., Shi, J., 2003. Application of a fractal method relating concentrations and distances for separation of geochemical anomalies from background. J. Geochem. Explor. 77, 167–175.
Lima, A., De Vivo, B., Cicchella, D., et al., 2003. Multifractal IDW interpolation and fractal filtering method in environmental studies: an application on regional stream sediments of (Italy), Campania region. Appl. Geochem. 18, 1853–1865.
Lima, A., De Vivo, B., Tarvainen, T., et al., 2008. Interpolation methods for geochemical maps: a comparative study using arsenic data from European stream waters. Geochemistry: Explor. Environ. Anal. 8, 41–48.
Mandelbrot, B.B., 1977. Fractals: Form, Chance, and Dimension. Freeman, San Francisco. 365.
Mandelbrot, B.B., 1983. The Fractal Geometry of Nature, (updated and augmented edition). Freeman, New York. 468.
Mandelbrot, B.B., Passoja, D.E., Paullay, A.J., 1984. Fractal character of fracture surfaces of metals. Nature 308 (5961), 721–722.
Miesch, A.T., 1981. Estimation of the geochemical threshold and its statistical significance. J. Geochem. Explor. 16, 49–76.
Qu, X., Hou, Z., Huang, W., 2001. Is Gangdese porphyry copper belt the second "Yulong" copper belt? Miner. Depos. 20, 355–366 (In Chinese with English abstract).
Qu, X., Hou, Z., Li, Y., 2004. Melt components derived from a subducted slab in late orogenic ore-bearing porphyries in the Gangdese copper belt, southern Tibetan plateau. Lithos 74, 131–148.
Raines, G.L., 2008. Are fractal dimensions of the spatial distribution of mineral deposits meaningful? Nat. Resour. Res. 17, 87–97.
Sanderson, D.J., Roberts, S., Gumiel, P., 1994. A fractal relationship between vein thickness and gold grade in drill core from La Codosera, Spain. Econ. Geol. 89, 168–173.
Shi, J., Wang, C., 1998. Fractal analysis of gold deposits in China: implication for giant deposit exploration. Earth Science -J. China Univ. Geosci. 23, 616–618 (In Chinese with English Abstract).
Sinclair, A.J., 1974. Selection of thresholds in geochemical data using probability graphs. J. Geochem. Explor. 3, 129–149.
Sinclair, A.J., 1976. Application of probability graphs in mineral exploration. Assoc. Explor. Geochem. Spec 4, 95.
Sinclair, A.J., 1991. A fundamental approach to threshold estimation in exploration geochemistry: probability plots revisited. J. Geochem. Explor. 41, 1–22.
Stanley, C. R., 1988. Comparison of data classification procedures in applied geochemistry using Monte Carlo simulation. Unpublished Ph.D. Thesis, Univ. of British Columbia, Vancouver, pp. 256.
Stanley, C.R., Sinclair, A.J., 1989. Comparison of probability plots and gap statistics in the selection of threshold for exploration geochemistry data. J. Geochem. Explor. 32, 355–357.
Turcotte, D.L., 1996. Fractals and Chaos in Geophysics, 2nd ed. Cambridge University Press, Cambridge U K, pp. 81–99.
Turcotte, D.L., 2002. Fractals in petrology. Lithos 65, 261–271.
Wang, Z., Cheng, Q., Cao, L., et al., 2006. Fractal modelling of the microstructure property of quartz mylonite during deformation process. Math. Geol. 39, 53–68.
Wang, Z., Cheng, Q., Xu, D., et al., 2008. Fractal modeling of sphalerite banding in Jinding Pb–Zn deposit, Yunnan, Southwestern China. J. China Univ. Geosci. 19, 77–84.
Xie, X., Mu, X., Ren, T., 1997. Geochemical mapping in China. J. Geochem. Explor. 60, 99–113.
Zuo, R., Xia, Q., Tan, N., et al., 2007. Synthetic information prediction of porphyry copper in Tibet. Central South University of Technology 38, 368–373 (In Chinese with English abstract).

Please cite this article as: Zuo, R., et al., Application of singularity mapping technique to identify local anomalies using stream sediment geochemical data, a case study from Gangdese, Tibet, western China, J. Geochem. Explor. (2008), doi:10.1016/j.gexplo.2008.08.003